Classical dimers on the triangular lattice

P. Fendley,[1] R. Moessner,[2] and S. L. Sondhi[3]
[1]*Department of Physics, University of Virginia, Charlottesville, Virginia 22904-4714*
[2]*Laboratoire de Physique Théorique de l'Ecole Normale Supérieure, CNRS-UMR8541, Paris, France*
[3]*Department of Physics, Princeton University, Princeton, New Jersey 08544*
(Received 22 June 2002; published 13 December 2002)

We study the classical hard-core dimer model on the triangular lattice. Following Kasteleyn's fundamental theorem on planar graphs, this problem is soluble using Pfaffians. This model is particularly interesting for, unlike the dimer problems on the bipartite square and hexagonal lattices, its correlations are short ranged with a correlation length of less than one lattice constant. We compute the dimer-dimer and monomer-monomer correlators, and find that the model is deconfining: the monomer-monomer correlator falls off exponentially to a constant value $0.1494\ldots$, only slightly below the nearest-neighbor value of 1/6. We also consider the anisotropic triangular lattice model in which the square lattice is perturbed by diagonal bonds of one orientation and small fugacity. We show that the model becomes noncritical immediately and that this perturbation is equivalent to adding a mass term to each of two Majorana fermions that are present in the long wavelength limit of the square lattice problem.

DOI: 10.1103/PhysRevB.66.214513 PACS number(s): 74.20.Mn, 05.50.+q, 71.10.−w

I. INTRODUCTION

The study of classical dimer models—the statistical mechanics of hardcore dimer coverings of graphs—has a venerable history. These models have been of interest as direct representations of the physics, e.g., diatomic molecules on a lattice but even more because of their equivalence to various other statistical mechanical problems; for example, the two-dimensional Ising model can be reformulated as a dimer model on a special lattice.[1,2] The reduction to dimer form is advantageous in that a wide class of dimer models, those on planar graphs with independent fugacities on bonds, are soluble by Pfaffians following a theorem of Kasteleyn[1] (also see Ref. 3). This technique has been applied to compute a variety of correlation functions, in the dimer model on the square lattice[4] and in the Ising model.[5]

The interest in dimer models has received new and very different impetus following the discovery of high-temperature superconductivity. Following Anderson's proposal[6] that the superconducting state evolves out of a liquid of singlet (valence) bonds, Rokhsar and Kivelson (RK) proposed a *quantum* dimer model[7] to describe this so-called short-range resonating valence bond (RVB) physics. The Hilbert space of their model consists of all pairings of the spins on the square lattice into singlet bonds; these can simply be labeled by hardcore dimer coverings. The quantum dynamics provides off-diagonal matrix elements between these coverings. This idea can be generalized to other lattices.

The properties of the classical dimer model enter the solution of such quantum dimer models in two ways. First, trivially but usefully, the infinite temperature statics of the quantum problem are given precisely by the classical problem with equal fugacities. Second, non-trivially and even more usefully, quantum dimer models generically exhibit a ''RK'' point—which generalizes Rokhsar and Kivelson's construction on the square lattice—where the quantum wavefunction is an equal amplitude superposition of dimer coverings which is the paradigmatic RVB form. Static, dimer diagonal, ground state correlations at the RK point are then again given by the correlations of the classical dimer model.[7,8] For the square lattice, the known results on the classical problem[4] showed that the quantum dimer model was critical at the RK point, which thus turned out to be an isolated critical point between two solid phases, rather than a representative of an RVB phase. A similar behavior occurs on the honeycomb lattice, where the classical model is equivalent to the five-vertex model on the square lattice.[10]

In recent work, two of the present authors showed that the triangular lattice leads to a a different outcome[9] with a RVB *phase*, including the RK point, characterized by liquid correlations. It was also noted that the model exhibits ''topological order'' in the sense of Wen[11] (ground state degeneracies on closed surfaces in the absence of symmetry breaking) characteristic of an Ising gauge theory.[9,12] As part of this work it was necessary to solve the isotropic classical dimer model on the triangular lattice and show that the dimer correlations were short-ranged. As this does not appear to have been done previously, with the exception of results for the thermodynamic limit entropy,[13–17] we have carried out a fuller analysis of the problem in this paper.

Two aspects of this expanded analysis are noteworthy. First, we show that monomers are deconfined on the triangular lattice. A monomer is a site which does not have a dimer touching it, and the classical monomer-monomer correlator is the ratio of the number of configurations with the two monomers to the number without them. Monomers are deconfined if this ratio approaches a constant, nonzero value as the distance between the two increases. In the quantum dimer model, two monomers have the interpretation of two ''test spinons'' obtained by breaking a valence bond apart into its constituent spins. Hence our result proves that spinons are deconfined at high temperatures in the triangular lattice quantum dimer model.[18,19] Second, we study the interpolation between the critical square lattice and the non-critical triangular lattice by tuning the fugacity for one species of bond. The diverging correlation length near the

former allows a continuum limit to be taken and yields a theory of two Majorana fermions with the monomer operator being identified with a linear combination of the spin operators in the two sectors.

We begin by computing the partition function for general fugacities and show that the model undergoes phase transitions only when it reduces to the square lattice model. Correspondingly, it exhibits long-ranged dimer correlations in the square lattice limit. Next we derive asymptotic forms for the Green function and dimer correlations which show that the correlation length is less than a lattice constant at the isotropic point. We extend the analysis to obtain the correlation length everywhere along the interpolation to the square lattice. In Sec. IV we turn to computing the free energy of two monomers in a background of dimers. We show that it falls off exponentially to a constant, proving that spinons are deconfined in the quantum dimer model at infinite temperature. In Sec. V we show that the continuum formulation of the critical square lattice problem is a theory of two Majorana fermions. The addition of the remaining bonds of the triangular lattice is equivalent to adding a mass term for each fermion and hence a transition of the Ising universality class. We end with some concluding remarks and two technical Appendixes.

II. MODEL AND PARTITION FUNCTION

A dimer is a bond connecting two nearest neighbors on a lattice. We study the close-packed model with hard cores, where an allowed dimer configuration has the property that each site of the lattice is paired with exactly one of its nearest neighbors, such a pair being denoted by a dimer placed on the link between the two sites. In the simplest form of the model, each dimer has the same fugacity; as the number of dimers is the same in all configurations, the correlations of the dimer model are thus given as the equally-weighted average over all possible dimer configurations. In the following, we will include unequal fugacities, so that the average to be taken then includes nontrivial weighting factors.

The close-packed hard-core dimer model can solved on any planar lattice by using Pfaffian techniques. (A planar graph contains no overlapping links.) These techniques were introduced in the early 1960s by Kasteleyn,[1] and Fisher and co-workers.[4,20,21] The result is simple to describe: on a planar graph one places arrows on the links so that each plaquette is ''clockwise odd,'' that is to say that the product of the orientations of the arrows around any even-length elementary plaquette traversed clockwise is odd. The antisymmetric matrix M_{ij} is then defined with $M_{ij}=1$ if an arrow points from point i to point j, $M_{ij}=-1$ if the arrow points from j to i, and $M_{ij}=0$ if i and j are not nearest neighbors. Kasteleyn's theorem states that for any planar graph M can be found, and that the number of dimer coverings (the partition function) is given by the Pfaffian of the matrix M:

$$Z=\pm \mathrm{Pf}[M].$$

The $\pm$ sign is chosen to make Z positive; henceforth we will omit this sign. This result is exceptionally useful because the Pfaffian is the square root of the determinant:

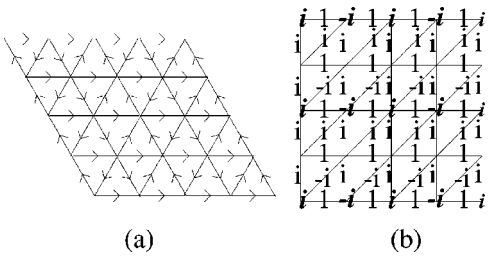

(a) (b)

FIG. 1. Choice of M for the triangular lattice. (a) A ''clockwise odd'' sign convention. (b) By multiplying the Grassmann variables on the sites by the phases indicated (italics), one obtains the new values for the M_{ij} on the bonds. Bonds are in addition multiplied by a fugacity. Note that in both cases, the unit cell is doubled.

$$\mathrm{Pf}[M]=(\det[M])^{1/2}.$$

For regular lattices, this determinant can easily be computed by using Fourier transformation. This result has been reformulated in the more modern language of fermionic path integrals in Ref. 15. One places a Grassmann variable ψ_i on each site i of the lattice, and defines the action $S=\Sigma_{i<j}M_{ij}\psi_i\psi_j$. Then a basic result of Grassmannian integrals gives

$$Z=\int [\mathcal{D}\psi]\exp(S).$$

This form allows one easily to define different but equivalent M by rescaling the fermions.

For the triangular lattice, an appropriate choice of arrows is displayed in Fig. 1. To make contact with the work on the square lattice, we however choose a different convention. First, we deform the triangular lattice into a topologically (but not symmetry) equivalent square lattice. Second, we multiply the Grassmann variables on every other row by alternating factors of $\pm i$ so that the values of M_{ij} are given as in Fig. 1, where the weight is to be understood to be for a convention of arrows pointing to the right/upwards. Finally, in order to be able to interpolate between square and triangular lattice, we allow the fugacity of the diagonal bonds to be a variable t instead of 1. For completeness, we give fugacities v and u to horizontal and vertical bonds, respectively. Note that we must double the unit cell to contain two sites; in our convention, it is doubled in the vertical direction. Each site i is labeled by the location of its unit cell, $\mathbf{x}$, and its location in the basis, α, while the unit vectors between cells are $\hat{\mathbf{x}}$ and $\hat{\mathbf{y}}$. The two fermions in the unit cell located at $\mathbf{x}$ are thus denoted as $\psi_{\alpha,\mathbf{x}}$ with $\alpha=1,2$. In this form, the action is

$$S=\tfrac{1}{2}\sum_{\mathbf{x},\alpha}\sum_{\mathbf{y},\beta}M^{\alpha\beta}_{\mathbf{xy}}\psi_{\alpha,\mathbf{x}}\psi_{\beta,\mathbf{y}} \tag{1}$$

where $M^{\alpha\beta}_{\mathbf{xy}}=-M^{\beta\alpha}_{\mathbf{yx}}$. With periodic boundary conditions (or far away from the boundaries), we have $M^{\alpha\beta}_{\mathbf{xy}}=M^{\alpha\beta}(\mathbf{x}-\mathbf{y})$, where

$$M^{12}(0)=M^{21}(\hat{\mathbf{y}})=iu,$$

$$M^{11}(\hat{\mathbf{x}}) = M^{22}(\hat{\mathbf{x}}) = v,$$

$$M^{21}(\hat{\mathbf{x}}+\hat{\mathbf{y}}) = -M^{12}(\hat{\mathbf{x}}) = it.$$

Since the action is quadratic in terms of the fermions, the model can be solved by Fourier transformation. Our convention for Fourier transforms is

$$\tilde{f}(\mathbf{k}) = \sum_{\mathbf{x}} e^{i\mathbf{k}\cdot\mathbf{x}} f(\mathbf{x}).$$

The action is then

$$S = \frac{1}{2} \sum_{\mathbf{k},\alpha,\beta} \tilde{M}_{\mathbf{k}}^{\alpha\beta} \tilde{\psi}_{\mathbf{k},\alpha} \tilde{\psi}_{-\mathbf{k},\beta}, \tag{2}$$

where the two-by-two matrix $\tilde{M}_{\mathbf{k}}$ is

$$\tilde{M}_{\mathbf{k}} = \begin{pmatrix} 2iv \sin k_x & g(\mathbf{k}) \\ g^*(\mathbf{k}) & 2iv \sin k_x \end{pmatrix},$$

with[22]

$$g(\mathbf{k}) = i[u - te^{ik_x} - ue^{-ik_y} - te^{-i(k_x+k_y)}].$$

Finding the determinant and hence the Pfaffian is now simple, because in $\mathbf{k}$ space the action is expressed in terms of the 4×4 blocks

$$\begin{pmatrix} 0 & \tilde{M}_{\mathbf{k}} \\ \tilde{M}_{-\mathbf{k}} & 0 \end{pmatrix} \tag{3}$$

on the diagonal. Note that this matrix is antisymmetric as it must be, because $g^*(\mathbf{k}) = -g(-\mathbf{k})$. The entropy per site, $\mathcal{S}$, of the dimer coverings on a N-site lattice is then

$$\mathcal{S} = \frac{1}{N} \ln \mathrm{Pf}[M] = \frac{1}{4} \sum_{\mathbf{k}} \ln|\Delta(\mathbf{k})|, \tag{4}$$

where

$$\Delta(\mathbf{k}) \equiv \det[\tilde{M}_{\mathbf{k}}] = \det[\tilde{M}_{-\mathbf{k}}]$$
$$= -4v^2 \sin^2 k_x - 4u^2 \sin^2(k_y/2) - 4t^2 \cos^2(k_x + k_y/2).$$

For a system with periodic boundary conditions, one must sum over four different sectors, according to the winding of the dimer configuration.[1] In fermionic language, this corresponds to evaluating four Pfaffians, with symmetric and antisymmetric boundary conditions, and combining them as $Z = (-\mathrm{Pf}_{pp} + \mathrm{Pf}_{ap} + \mathrm{Pf}_{pa} + \mathrm{Pf}_{aa})/2$, where the subscripts denote the (anti)periodic boundary conditions for the fermions in the two directions. In a Fourier representation, this corresponds to the usual different choices of allowed wavevectors. We have listed the number of dimer coverings thus obtained for the isotropic case in Table I, along with the results for a system with open boundary conditions.

In the thermodynamic limit, the sum over $\mathbf{k}$ in Eq. (4) turns into an integral. For the isotropic triangular lattice ($t=u=v=1$), doing the integral numerically yields

TABLE I. Number of dimer coverings, Z, of triangular lattices of with $L_x \times 2L_y$ sites, with periodic and open boundary conditions. For periodic boundary conditions, only those sizes ($L_x \geqslant 3$ and $L_y \geqslant 2$) are given in which any pair of sites is linked by at most one bond.

L_x	L_y	Z_{open}	Z_{torus}
1	1	1	
2	1	2	
3	1	3	
4	1	5	
5	1	8	
6	1	13	
1	2	1	
2	2	5	
3	2	15	344
4	2	56	1920
5	2	203	10608
6	2	749	59040
1	3	1	
2	3	13	
3	3	85	4480
4	3	749	59040
5	3	6475	767776
1	4	1	
2	4	34	
3	4	493	58592
4	4	10293	1826944
1	5	1	
2	5	89	
3	5	2871	766528
1	6	1	
2	6	233	
3	6	16731	10028288

$$\mathcal{S} = 0.4286\ldots.$$

We note $\mathcal{S}$ has been obtained previously by several authors[13–17] in different contexts, including the kagome Heisenberg magnet[16] and, implicitly, the fully frustrated Ising model on the hexagonal lattice,[17] where the ground state entropy per spin $\mathcal{S}_{FFHIM} = \mathcal{S}/2$ is related to the dimer model entropy via a duality mapping.[12]

This model simplifies in several limiting cases. If two fugacities vanish, the model reduces to decoupled chains, with order along the chains and disorder relative to one another. More interesting is the case where one of the fugacities vanishes, the square-lattice dimer model. This model is critical, with algebraic decay of correlators.[4,23] It is straightforward to show that the entropy $\mathcal{S}(t,v,u)$ is nonanalytic in t at $t=0$ (and likewise for u and v). We will discuss this in more detail in Sec. V.

III. GREEN FUNCTION

We now turn our attention to the correlations of the triangular dimer model. We utilize the techniques developed for

the square lattice in Ref. 4, and expressed in terms of Grassmann variables in Ref. 15. Correlation functions can be straightforwardly expressed in terms of the Grassmann variables (see, e.g., Ref. 24). Since the action is quadratic, using Wick's theorem expresses all correlators in terms of the Green function

$$\langle \psi_i \psi_j \rangle = \frac{1}{Z} \int [\mathcal{D}\psi] \psi_i \psi_j \exp(S).$$

For example, the probability $P^{(d)}(\hat{\mathbf{j}})$ of finding a dimer on a bond in the $(\hat{\mathbf{j}})$ direction at site 0 is given by

$$P^{(d)}(\hat{\mathbf{j}}) = |\langle \psi_0 \psi_{\hat{\mathbf{j}}} \rangle|. \tag{5}$$

In the original matrix language, the Green function elements make up the inverse of the matrix M, namely,

$$\langle \psi_i \psi_j \rangle = (M^{-1})_{ji} = -(M^{-1})_{ij}.$$

In this section we explicitly determine the Green function and its asymptotic behavior. In Sec. IV we use these results to determine the dimer-dimer and monomer-monomer correlators.

As shown in Sec. II, in Fourier space the action is written in terms of the 4×4 blocks [Eq. (3)]. These blocks can be easily inverted to give the two-point functions in Fourier space. Expressed in terms of the functions $g(\mathbf{k})$ and $\Delta(\mathbf{k})$, we have

$$\langle \tilde{\psi}_{1,\mathbf{k}} \tilde{\psi}_{1,-\mathbf{k}} \rangle = \langle \tilde{\psi}_{2,\mathbf{k}} \tilde{\psi}_{2,-\mathbf{k}} \rangle = \frac{2i \sin(k_x)}{\Delta(\mathbf{k})},$$

$$\langle \tilde{\psi}_{1,\mathbf{k}} \tilde{\psi}_{2,-\mathbf{k}} \rangle = -\frac{g^*(\mathbf{k})}{\Delta(\mathbf{k})},$$

$$\langle \tilde{\psi}_{2,\mathbf{k}} \tilde{\psi}_{1,-\mathbf{k}} \rangle = -\frac{g(\mathbf{k})}{\Delta(\mathbf{k})}.$$

To determine the Green functions in real space, we need to invert the Fourier transform. This yields

$$\langle \psi_{\alpha,\mathbf{x}} \psi_{\beta,\mathbf{y}} \rangle = \int d\mathbf{k} e^{-i\mathbf{k}\cdot(\mathbf{x}-\mathbf{y})} \langle \tilde{\psi}_{\alpha,\mathbf{k}} \tilde{\psi}_{\beta,-\mathbf{k}} \rangle \tag{6}$$

where we define

$$\int d\mathbf{k} \equiv \frac{1}{4\pi^2} \int_0^{2\pi} dk_x \int_0^{2\pi} dk_y.$$

For a finite number of sites, this integral is replaced with the usual sum. To simplify the resulting expressions, we specialize slightly in the subsequent analysis

(1) We work in the thermodynamic limit so we have integrals over $\mathbf{k}$.

(2) We set $u=v=1$. Thus the fugacity t gives a way of interpolating between the square and the isotropic triangular lattices, with $t=0$ giving the former and $t=1$ the latter.

(3) We study correlators where the fermions are in the same or adjacent rows.

It is also convenient to absorb some factors of $\pm i$ by defining the Green functions Q_s and R_s as

$$\langle \psi_{1,\mathbf{x}} \psi_{1,\mathbf{x}+s\hat{\mathbf{x}}} \rangle = \langle \psi_{2,\mathbf{x}} \psi_{2,\mathbf{x}+s\hat{\mathbf{x}}} \rangle \equiv (-1)^{(s+1)/2} Q_s,$$

$$\langle \psi_{1,\mathbf{x}} \psi_{2,\mathbf{x}+s\hat{\mathbf{x}}} \rangle = -\langle \psi_{2,\mathbf{x}} \psi_{1,\mathbf{x}-s\hat{\mathbf{x}}} \rangle \equiv i(-1)^{[(s+1)/2]} R_s,$$

where $[a]$ is the greatest integer less than a. Relatively simple expressions for Q_s and R_s are obtained by shifting $k_x \to k_x + \pi/2$ and $k_y \to 2k_y + \pi$. For odd s,

$$Q_s = \int d\mathbf{k} w(k_x, k_y) \cos(k_x) \cos(s k_x), \tag{7}$$

$$R_s = t \int d\mathbf{k} w(k_x, k_y) \cos(k_x + k_y) \cos(s k_x + k_y), \tag{8}$$

while for even s,

$$Q_s = 0, \tag{9}$$

$$R_s = \int d\mathbf{k} w(k_x, k_y) \cos(k_y) \cos(s k_x + k_y), \tag{10}$$

where

$$w(k_x, k_y) = \frac{1}{2} \frac{1}{\cos^2(k_x) + \cos^2(k_y) + t^2 \cos^2(k_x + k_y)}.$$

These integrands are all invariant under the interchange of k_x and k_y, under $\mathbf{k} \to -\mathbf{k}$, and under shifts of π.

One of the two integrals in each of the Q_s and R_s can be done immediately by residue. We let $a = k_x + k_y$ and $b = k_x - k_y$ so that $w^{-1} = 2[1 + \cos(a)\cos(b) + t^2 \cos^2(a)]$. The integral over b can be deformed so that the contour runs around the pole at

$$\cos(b) = \frac{1 + t^2 \cos^2(a)}{\cos(a)}.$$

This is done by changing the integration contour running from $-\pi$ to π along the real axis to one which first runs from $-\pi$ to $-\pi + i\infty$, then to $+\pi + i\infty$, and finally back down to π. The two contours running parallel to the imaginary axis cancel as the function is periodic under $b \to b + 2\pi$, and the contribution from the contour running parallel to the real axis vanishes when the integrand vanishes exponentially as $\mathrm{Im}(b) \to \infty$. We thus pick up only the contribution of the pole of the integrand. For example, we have

$$\int_0^{2\pi} \frac{db}{2\pi} \frac{1}{1 + r\cos(b) + t^2 r^2} = \frac{1}{\sqrt{1 + (2t^2 - 1) r^2 + t^4 r^4}}.$$

The resulting expressions for Q_s and R_s are simpler on the isotropic triangular lattice $t=1$ because of the additional symmetry. In particular, here $w(k_x, k_y)$ is invariant under the transformation $k_x \to -(k_x + k_y)$; this ensures that the Green functions are invariant under a 60° rotations of the lattice. For example, this transformation allows us to change the numerator of Q_s from $\cos(sk_x)\cos(k_x)$ to $\cos(sa)\cos(a)$. This gives us

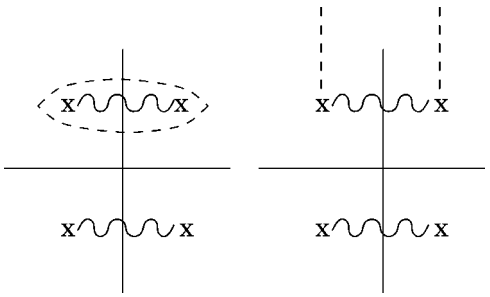

FIG. 2. The integration contours (dashed) used for the asymptotic evaluation of the Green function when $t>1/2$. The second is equivalent to the first if the integrand is multiplied by 2. For $t<1/2$, the branch cuts have $\mathrm{Re}(a)=0$.

$$Q_s(t=1)=\frac{1}{2\pi}\int_0^{\pi} da\,\frac{\cos(sa)\cos(a)}{\sqrt{1+\cos^2(a)+\cos^4(a)}}, \quad (11)$$

and for odd s

$$R_s(t=1)=\frac{1}{4\pi}\int_0^{\pi} da\frac{\cos(sa)e^{ib_0}+\cos[(s-1)a]}{\sqrt{1+\cos^2(a)+\cos^4(a)}} \quad (12)$$

while for even s,

$$R_s(t=1)=\frac{1}{4\pi}\int_0^{\pi} da\frac{\cos[(s-1)a]e^{ib_0}+\cos(sa)}{\sqrt{1+\cos^2(a)+\cos^4(a)}} \quad (13)$$

where

$$e^{ib_0}=\frac{1+\cos^2(a)-\sqrt{1+\cos^2(a)+\cos^4(a)}}{\cos(a)}.$$

A. Asymptotic long-distance behavior

In this subsection, we study the long-distance behavior of the Green functions Q_s and R_s. We derive an expression for the correlation length of the fermions at any t, and find that it indeed vanishes only when $t=0$.

Unlike the similar case of the square lattice, the integrals for the Green function cannot be evaluated asymptotically by partial integration. This method only works for algebraic correlations, whereas in our case, the correlations decay exponentially. One can nonetheless obtain the asymptotics by deforming the integration contour. Instead of there being poles in the complex a plane, there are now square-root branch cuts. In the region $|\mathrm{Re}(a)|<\pi/2$, there is one branch cut in the lower-half-plane and one in the upper. For $t<1/2$, the branch cut has $\mathrm{Re}(a)=0$, while for $t>1/2$, it is parallel to the $\mathrm{Re}(a)$ axis. The general formula for the location of the branch points $a_{\pm}$ is

$$\cos(a_{\pm})=\frac{1\pm\sqrt{1-4t^2}}{2t^2}. \quad (14)$$

For the same reason we could deform the b integral around the pole, we can now deform the a integral around the branch cut, as depicted in first part of Fig. 2. To evaluate the integral by saddle point, we want a contour where the e^{isa} term in the integrand is decreasing exponentially. It is thus easiest to use the fact that with a square-root branch cut, the integral around one side of the branch is equal to the integral around the other. Thus the contour can be deformed yet again, so that it goes from the two branch points to $i\infty$, as long as we multiply the result by 2. This contour, denoted by $\mathcal{C}$, is depicted in the second part of Fig. 2.

With this new contour, asymptotic evaluation of the integral is easy, because the integrands are sharply peaked at the branch points. For example, we have

$$Q_s(t=1)=\frac{1}{2\pi}\int_{\mathcal{C}} da\frac{e^{i(s+1)a}+e^{i(s-1)a}}{\sqrt{1+\cos^2(a)+\cos^4(a)}}.$$

The exponentials rapidly decrease as $\mathrm{Im}(a)$ is increased along the contour, and moreover, the rest of the integrand has a square-root divergence at the branch points. It is thus an asymptotically exact approximation to substitute $\sqrt{1+\cos^2(a)+\cos^4(a)}\approx C\sqrt{a-a_{\pm}}$ into the integrand. This gives

$$Q_s(t=1)\approx f(|s+1|)+f(|s-1|), \quad (15)$$

where

$$f(s)\equiv \mathrm{Re}\left[\frac{1}{\sqrt{C}\pi}\int_{a_+}^{i\infty} da\,\frac{e^{-isa}}{\sqrt{a-a_+}}\right].$$

We have used the fact that the integral from a_- to infinity is the complex conjugate of the integral from a_+ to infinity. After shifting $a\to a+a_+$, the integral is easily done, yielding

$$f(s)=\mathrm{Re}\left[\frac{1}{\sqrt{Cs\pi}}e^{ia_+s}\right].$$

Finally, we break a_+ into its real and imaginary parts: $a_+=\alpha+i\beta$. For $t=1$, $\cos(a_+)=\exp(2i\pi/3)$, so that $C=3^{3/4}2\exp(-i\pi/4)$, $\alpha=1.1960\ldots$ and

$$\beta=\frac{1}{4}\ln\left[\frac{\sqrt{2}+3^{1/4}}{\sqrt{2}-3^{1/4}}\right]=0.83144\ldots. \quad (16)$$

Plugging this in gives

$$f(s)=\frac{1}{\sqrt{2\pi 3^{3/4}}}\frac{e^{-\beta s}}{\sqrt{s}}\cos\left(\alpha s+\frac{\pi}{8}\right). \quad (17)$$

The asymptotic expression for R_s can now easily be found by noticing that at the branch point $a=a_+$, $e^{ib_0}=-1$. This means that

$$R_s(t=1)\approx(-1)^s[f(|s|)-f(|s-1|)]. \quad (18)$$

We have therefore shown that on the isotropic triangular lattice, β is the inverse correlation length along the rows. It is only about one lattice spacing, so the exponential decay of the Green functions is quite rapid. Comparing the asymptotic form to the exact values derived in Sec. III B (see Fig. 3 for a plot of Q_s), one finds that the agreement is excellent—

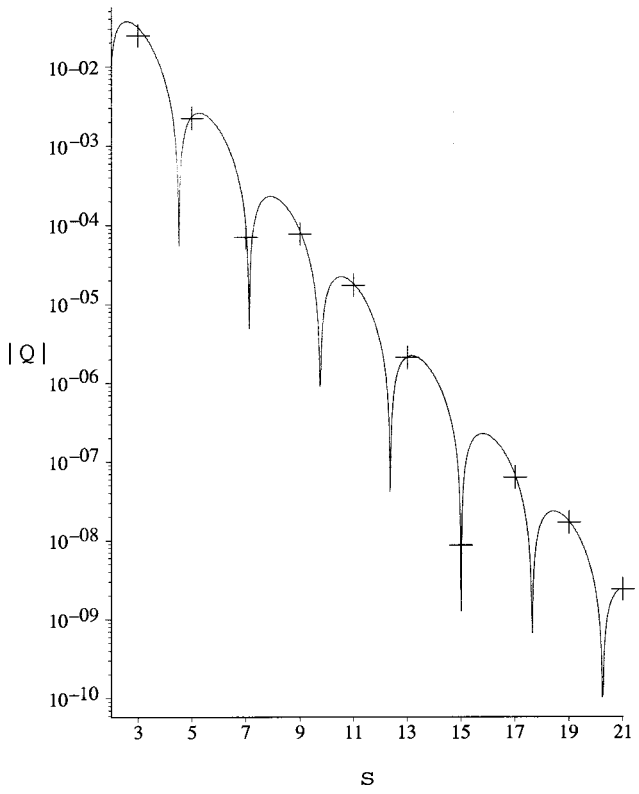

FIG. 3. The curve is the asymptotic expression for $|Q_s|$ when $t=1$ [Eq. (15)]. The points are the exact values at odd s; Q_s vanishes for even s.

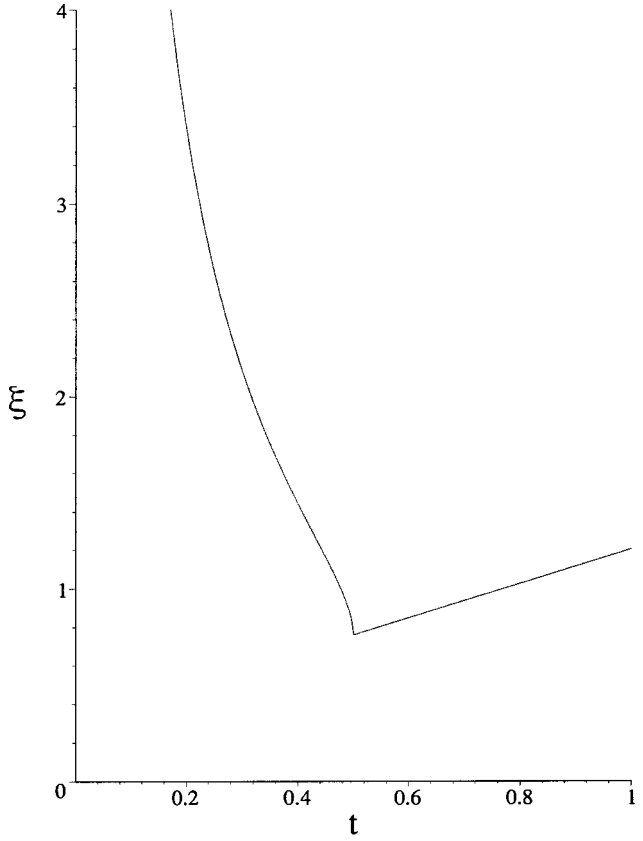

FIG. 4. The correlation length as a function of the dimer fugacity: $t=0$ is the square lattice, $t=1$ the isotropic triangular lattice.

within a few percent—even for small values of s. At occasional values of s (e.g., $s=15$); however, the agreement is only within a factor of 2 or so. The reason is that the oscillating factor in Eq. (17) occasionally becomes very close to zero near s an odd integer, so that the terms we have neglected above can become larger than the one we kept. This however, does not change our results for the correlation length, because the neglected terms have the same exponential dependence on s [but a power law exponent different from $-1/2$ in Eq. (17)].

For arbitrary t, the computations are similar but the equations look fairly gruesome. Finding asymptotic expressions for Q_s and R_s is more complicated because the transformation $k_x \to -(k_x+k_y)$ no longer leaves $w(k_x,k_y)$ invariant. However, we can easily extract the correlation length for Green functions in the $\hat{\mathbf{x}}+\hat{\mathbf{y}}$ direction (the direction along the links with t-dependent fugacity). The reason is that the expressions for the Green functions in this direction end up very similar to Eqs. (12) and (13). The key fact is that there are no terms in the integrand involving e^{isb_0}, only e^{ib_0}. Like before, the integrand is peaked around the branch points given in Eq. (14). Thus the fermion correlation length $\xi^{\hat{\mathbf{x}}+\hat{\mathbf{y}}}$ is given by

$$(\xi^{\hat{\mathbf{x}}+\hat{\mathbf{y}}})^{-1} = \mathrm{Im}\left[\arccos\left(\frac{1-\sqrt{1-4t^2}}{2t^2}\right)\right]. \tag{19}$$

We plot this correlation length in Fig. 4. Note that the kink at $t=1/2$ in Fig. 4 is evidence of a level crossing between two eigenvalues of the triangular lattice.

As $t\to 0$, the correlation length diverges as $1/t$,

$$\xi^{\hat{\mathbf{x}}+\hat{\mathbf{y}}} \approx \frac{1}{\sqrt{2}t}, \quad t\to 0,$$

while $\xi = 1/\beta = 1.2027\ldots$ at $t=1$. In this expression, we have taken the length of a diagonal bond as unit distance. Translating this back into square-lattice language (with the length unit given by a lattice constant) removes the factor of $1/\sqrt{2}$. The diverging correlation length in the square lattice limit will be used to take a continuum limit in Sec. V below.

B. Short-distance behavior on the isotropic lattice

In this subsection we show how to derive exact expressions for the Green functions on the isotropic triangular lattice, $t=1$. We start by noting that a few of these Green functions can be evaluated immediately. In the isotropic case, the probability of a dimer being on a given link is 1/6. This is of course related to the Green function for neighboring fermions by Eq. (5), so

$$Q_1 = R_1 = R_0 = \frac{1}{6}.$$

Ironically, this fact is not easy to extract from the explicit integrals [Eqs. (11)–(13)]. It does follow from noting that the

TABLE II. The Green function Q_s explicitly.

s	Q_s	Numerical value
1	$1/6$	0.16666666666666666667
3	$-1/2+1/6\frac{\sqrt{3}}{U_0\pi}$	−0.024550581458226763328
5	$8U_0+5/6-5/6\frac{\sqrt{3}}{U_0\pi}$	0.002213263243038304 3346
7	$-56U_0+\frac{25}{6}+7/3\frac{\sqrt{3}}{U_0\pi}$	0.000069367921493899 5513
9	$216U_0-\frac{93}{2}+5/3\frac{\sqrt{3}}{U_0\pi}$	−0.000076203880846465563
11	$-\frac{1288}{5}U_0+\frac{1397}{6}-\frac{385}{6}\frac{\sqrt{3}}{U_0\pi}$	0.000017066432646044 3169
13	$-\frac{16016}{5}U_0-\frac{3443}{6}+\frac{2509}{6}\frac{\sqrt{3}}{U_0\pi}$	−0.000002068500172729645
15	$29232U_0-\frac{2885}{2}-\frac{30970}{21}\frac{\sqrt{3}}{U_0\pi}$	0.000000008625529538 7778

transformation $k_x\rightarrow-(k_x+k_y)$ in Eqs. (7),(8), and (10) means that $Q_1=R_1=R_0$, and also that $Q_1+R_1+R_0=1/2$.

By generalizations of this argument, it is possible to derive recursion relations relating Q_s and R_s. For the square lattice they are discussed in Ref. 23. For the isotropic triangular lattice, the relations relating all the R_s's to the Q_s's can be derived using simple trigonometric identities. One finds here that

$$R_{2j+2}=R_{2j+1}-R_{2j}+R_{2j-1}+Q_{2j+1}-Q_{2j-1}$$

and

$$2R_{2j+1}=-2R_{2j}-Q_{2j+1}-Q_{2j-1}+\delta_{j0}.$$

The Kronecker delta in the latter identity arises from the integral $\int d\mathbf{k}\cos(jx)=\delta_{j0}$. The recursion relations involving only Q_s are trickier to obtain; we discuss them in the Appendixes.

The recursion relations mean that Q_s and R_s for any s can be expressed in terms of Q_1, R_2, and Q_3. These in turn can be evaluated in terms of elementary functions; in particular the combination

$$U_0=\frac{\Gamma(7/6)}{2\Gamma(2/3)\sqrt{\pi}}. \tag{20}$$

As detailed in Appendix A, along with $Q_1=1/6$ we have

$$R_2=\frac{1}{3}-2U_0,$$

$$Q_3=-\frac{1}{2}+\frac{1}{6}\frac{\sqrt{3}}{U_0\pi}.$$

Using these facts, we can evaluate the Green functions to arbitrarily good accuracy numerically by using, e.g., Maple. Although it is easy to iterate the recursion relations on the computer, we have not succeeded in finding a closed-form expression for arbitrary Q_s and R_s. We have collected some of them in Table II. Note that even though the coefficients are increasing exponentially with s, the three terms in each cancel almost perfectly to give the exponential falloff in s.

IV. CORRELATORS

A. Dimer-dimer correlation function

The dimer-dimer correlation function is easily expressed in terms of the Green functions. The operator $\psi_{1,\mathbf{x}}\psi_{2,\mathbf{x}}$ creates a dimer at site $\mathbf{x}$ pointing in the $\hat{\mathbf{y}}$ direction. The probability that there are two parallel dimers in the same row a distance s apart is therefore

$$P^{(dd)}(s)=\langle\psi_{1,\mathbf{x}}\psi_{2,\mathbf{x}}\psi_{1,\mathbf{x}+s\hat{\mathbf{x}}}\psi_{2,\mathbf{x}+s\hat{\mathbf{x}}}\rangle.$$

By Wick's theorem, this decomposes into

$$P^{(dd)}(s)=(R_0)^2-(Q_s)^2-R_sR_{-s}.$$

This, therefore, decays exponentially to its asymptotic value with half the correlation length of the Green function. For the isotropic lattice, one can easily plug in the asymptotic forms [Eqs. (15) and (18)] derived in Sec. III, and find the correlation length $1/(2\beta)\approx0.6014$, less than one lattice spacing.

B. Monomer-monomer correlation function

As noted in Sec. I, the asymptotic behavior of the monomer-monomer correlation function is quite interesting physically. A zero value means the model is confining, while a nonzero value means that the model is in a deconfined phase. We will show in this subsection that on the isotropic triangular lattice, the latter is true.

A monomer placed on a lattice site forbids a dimer from being placed on any of the links connected to the site. The monomer-monomer correlator $P^{(mm)}(q,r)$ is the ratio of the number of configurations with monomers at sites q and r to the number of configurations without the monomers. Thus computing a monomer-monomer correlator follows from the partition function of the lattice with the two sites (and all the links connected to these sites) deleted. Since such a lattice is planar, Kasteleyn's construction is still applicable. The one complication is that we must ensure that on the lattice with deleted sites, the number of arrows is still clockwise odd. With the assignment in Fig. 1, one sees immediately that the number of arrows around a deleted site is even. Thus this assignment must be modified by reversing one of the arrows in the plaquette around the deleted site. Reversing the arrow on this link then ruins the clockwise-odd assignment around the other plaquette this link borders. Thus we must reverse one of the other arrows on this other plaquette. This in turn ruins another assignment, and so on. We thus must build up a string of reversed arrows, which must stretch from one monomer to the other. As long as the arrows are chosen to make all plaquettes clockwise odd, the monomer correlator is independent of the choice of path of the string. For monomers in adjacent rows, this construction is illustrated in Fig. 5; links with the thick lines are part of the string.

This is very much like constructing the spin-spin correlation function in the Ising model in terms of fermionic variables. In fact, on the square lattice, the monomer-monomer

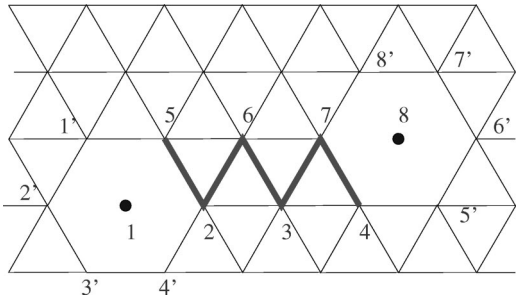

FIG. 5. The string in the monomer-monomer correlator with $p=4$.

correlator was shown[4,23] to have the same long-distance behavior (falloff as the square root of the distance) as the spin-spin correlation function in two decoupled Ising models. The precise relation between the two correlators for the square lattice was given in Ref. 25. In Sec. V, we will extend this relation away from the square lattice.

We define as the monomer-monomer correlation function $P^{(mm)}$ as the ratio of the number of configurations with the monomers to the number without. This can be written in terms of the fermions. Deleting a site merely corresponds to inserting a fermion at that site. Changing the sign of the arrow corresponds to changing the sign of the term of the fermion in the action. In our theory with action $\Sigma_{j<k} M_{jk}\psi_j\psi_k$, for a monomers at sites q and r,

$$P^{(mm)}(q,r)=\left|\left\langle \psi_q \prod\ (1-2M_{ab}\psi_a\psi_b)\psi_r\right\rangle\right| \qquad (21)$$

where the product is over all the links connecting sites q and r which have reversed arrows. We specialize to the case of one monomer being at the origin and the other in an adjacent row p lattice spacings apart, as illustrated in Fig. 5. Labeling the fermions in the lower row $1\ldots p$ and those in the upper row as $p+1\ldots 2p$ gives

$$P^{(mm)}(p)=|\langle \psi_1(1-2i\psi_{p+1}\psi_2)(1+2it\psi_2\psi_{p+2}) \ldots(1-2i\psi_{2p-1}\psi_p)\psi_{2p}\rangle|. \qquad (22)$$

Since the theory is free in terms of the fermions, one can use Wick's theorem to express this correlator as a product of Green functions. Evaluating it by brute force, however, is too difficult for all but low values of p, because the number of contractions grows exponentially. For a two-site separation,

$$P^{(mm)}(2)=R_2(1-R_0)-2R_1^2-2Q_1^2.$$

Using the results of the previous section for the Green functions, one has, for $t=1$,

$$P^{(mm)}(2)=4U_0/3-1/9=.14657672599\ldots\ .$$

To proceed further, one must in revert to the Pfaffian methods developed for the square lattice.[4] Our calculation generalizes these methods to the triangular lattice. The monomer-monomer correlator [Eq. (22)] can be expressed in Pfaffian language as

$$P^{(mm)}=\frac{\mathrm{Pf}(M^{(mm)})}{\mathrm{Pf}(M)}$$

where $M^{(mm)}$ is the Kasteleyn matrix with the monomer sites removed, and the signs reversed on the links of the string connecting the monomers. The advantage of this formulation is that one can manipulate a matrix without changing the determinant. For example, if one adds any row of a matrix to any other row, the determinant is left unchanged. Thus the strategy is to find explicitly the matrix $M^{-1}M^{(mm)}$ describing the monomer correlator, and manipulate it to make it more tractable.[4] On the square lattice, it is simple to show that

$$\det(M^{-1}M^{(mm)})=\det(T)^2,$$

where T is a $p\times p$ matrix. After a variety of manipulations described in appendix B, one finds the same behavior on the triangular lattice.

Deferring the details to Appendix B, our result is that the monomer-monomer correlator is

$$P^{(mm)}(p)=\frac{1}{2}\det(\mathcal{R}+\mathcal{Q}). \qquad (23)$$

where the entries of the $p\times p$ matrices $\mathcal{Q}$ and $\mathcal{R}$ are

$$\mathcal{R}_{ij}=(-1)^{[(j-i)/2]}R_{j-i+1}+t^{i-j-1}\theta(i-j), \qquad (24)$$

$$\mathcal{Q}_{ij}=i(-1)^{[(j+i)/2]}Q_{p+1-i-j}, \qquad (25)$$

where $\theta(x)=1$ for $x>0$ and 0 for $x\leqslant 0$. Unlike the case of the square lattice, the matrix $\mathcal{R}+\mathcal{Q}$ is not Toeplitz (the entries in a Toeplitz matrix T_{ij} depend only on $i-j$). For Toeplitz matrices, Szego's theorem provides a simple way of finding the asymptotic behavior of the determinant as the matrices get large. Here, $\mathcal{R}_{ij}$ depends only on $i-j$, but $\mathcal{Q}_{ij}$ depends only on $i+j$. We do not know if there is a generalization of Szego's theorem to our case.

To evaluate this correlator for $t=1$, we can plug the Green functions derived in Sec. III into the expression for $P^{(mm)}$ [Eq. (23)]. Expressing them in terms of U_0 as before, the final form of the determinant simplifies substantially (although it is still fairly horrible). For example, for $p=3$ one finds

$$P^{(mm)}(3)=\frac{\sqrt{3}+(2\pi-3\sqrt{3})U_0-144\pi U_0^3+864\pi U_0^4}{27\pi U_0}.$$

We have collected some numerical values in Table III. The correlator falls off exponentially to the value

$$P^{(mm)}(\infty)=0.14942924536134225401731517482693\ldots\ .$$

So the monomers clearly are deconfined in this phase, since the monomer one-point function $[\equiv\sqrt{P^{(mm)}(\infty)}]$ is nonvanishing. Numerically, one can check that the correlation length here is the same as for the dimer-dimer correlation, namely, $1/(2\beta)$, or about 0.6 of a lattice spacing.

TABLE III. The monomer-monomer correlation function for the isotropic triangular lattice.

s	$P^{(mm)}(s)$
1	0.16666666666666666666667
2	0.14657672599198408128222 0
3	0.15026355803697611860462 4
4	0.14935452895780982673308 4
5	0.14944115728626065006223 7
6	0.14943010503134845596963 7
7	0.14942909110538665435985 1
8	0.14942931237674296692541 4
9	0.14942924312362045247044 6
10	0.14942924548355826574155 5
11	0.14942924569149577085135 0
12	0.14942924531921209774791 8
13	0.14942924537112532889203 8
14	0.14942924536158195994052 3
15	0.14942924536125664597393 0

C. Vison-vison correlation function

In the quantum dimer model, a π-flux vortex or ''vison''[26,27] involves a semi-infinite string on the dual lattice. A particular dimer configuration c acquires a factor of $(-1)^{N_{\text{string}}(c)}$, where $N_{\text{string}}(c)$ is the number of dimers intersecting that string. For two visons separated by $\mathbf{x}$ the string can be taken to run from one vison to the other and hence no flux is visible at infinity. At the RK point, the calculation of the static two vison correlator reduces to the evaluation of $\Sigma_c(-1)^{N_{\text{string}(0,\mathbf{x})}(c)}$ which is now a purely classical problem. We will henceforth refer to this sum and its generalizations to unequal fugacities as the two-vison correlator even though the latter do not correspond to any known quantum problem. We should also note that the choice of string, which needs to be made for each separation, lead to an ambiguity of a sign at each separation.

The two-vison correlator was studied recently in Ref. 28 for a Kagome spin problem equivalent to a generalized dimer model on the triangular lattice requiring three dimers per site. There are some special features of this problem, arising from the ''particle-hole'' symmetry of occupying three dimers out of a possible six at each site and among them is the presence of two species of visons (for details the reader should consult the original work). In our problem, that of one dimer per site on the triangular lattice, life is simpler. Here the two-vison correlator can be seen, most simply by duality arguments described in Appendix A of Ref. 12, to be equal in magnitude (we have already commented on the sign ambiguity) to the spin-spin correlation function averaged over the ground state manifold of the fully frustrated Ising model on the honeycomb lattice. The latter is known, and decays exponentially with a correlation length computed in Ref. 17. A direct computation of the vison correlator is in progress[29] and should obviate the need for the detour we have taken in this section.

V. PERTURBING ABOUT THE SQUARE LATTICE: FIELD THEORY

As we noted earlier, the general triangular lattice dimer model is critical in the square lattice limit. This suggests that we can gain some insight into its properties by considering a continuum limit when the diagonal fugacity t is small. We should immediately enter one caveat: our exact computation shows that there is a level crossing in the excited state spectrum of the transfer matrix (the kink in Fig. 4) *en route* from the square lattice to the isotropic triangular lattice so there are details of the latter that the continuum theory will not reproduce very well.

Returning to the fermion action and setting $t=0$, it turns out that in the absence of diagonal bonds we no longer need to double the unit cell as was necessary for in Eq. (3); the fermion operators ψ_i used in this section thus refer to the sites $\mathbf{x}$ of the square lattice.

In momentum space, the resulting action is given by

$$S_0=\frac{1}{2}\sum_k (2i\sin k_x-2\sin k_y)\tilde{\psi}_{\mathbf{k}}\tilde{\psi}_{-\mathbf{k}}, \tag{26}$$

where we have now reverted to the standard Euclidean field theory convention of including an explicit minus sign with the action in writing down the Grassmann integral. We see that the fermion dispersion has nodes at $\mathbf{k}=(0,0)$, $(0,\pi)$, $(\pi,0)$, and (π,π). Linearizing near these points and defining

$$\begin{aligned}
\tilde{\chi}^1_{\mathbf{k}}&=\tilde{\psi}_{\mathbf{k}},\\
\tilde{\chi}^{\bar{1}}_{\mathbf{k}}&=\tilde{\psi}_{\pi\hat{\mathbf{y}}+\mathbf{k}},\\
\tilde{\chi}^2_{\mathbf{k}}&=i\tilde{\psi}_{\pi(\hat{\mathbf{x}}+\hat{\mathbf{y}})+\mathbf{k}},\\
\tilde{\chi}^{\bar{2}}_{\mathbf{k}}&=i\tilde{\psi}_{\pi\hat{\mathbf{x}}+\mathbf{k}},
\end{aligned} \tag{27}$$

we obtain the long wavelength form ($\partial\equiv\frac{1}{2}\partial_x-i\partial_y$, $\bar{\partial}\equiv\frac{1}{2}\partial_x+i\partial_y$)

$$S_0=2\int d^2\mathbf{x}(\chi^1\bar{\partial}\chi^1+\bar{\chi}^{\bar{1}}\partial\bar{\chi}^{\bar{1}}+\chi^2\bar{\partial}\chi^2+\bar{\chi}^{\bar{2}}\partial\chi^2), \tag{28}$$

which is a theory of two Majorana fermions, both holomorphic (χ^1,χ^2) and antiholomorphic $(\bar{\chi}^{\bar{1}},\bar{\chi}^{\bar{2}})$ fields. The labels 1 and 2 here are not the same as those used to label the two fermions in the unit cell; now the variables x and y run over all sites.

The leading asymptotic behavior of the lattice Green function can be recovered by inverting Eq. (27),

$$\begin{aligned}
\psi(\mathbf{x})=&\chi^1(\mathbf{x})+(-1)^y\bar{\chi}^{\bar{1}}(\mathbf{x})+i(-1)^{x+y+1}\chi^2(\mathbf{x})\\
&+i(-1)^{x+1}\bar{\chi}^{\bar{2}}(\mathbf{x}),
\end{aligned}$$

and using the continuum correlators

$$\langle\chi^a(\mathbf{x})\chi^a(0)\rangle=\frac{1}{4\pi}\frac{1}{x+iy},$$

$$\langle \chi^a(\mathbf{x})\chi^a(0)\rangle = \frac{1}{4\pi}\frac{1}{x-iy}$$

for $a=1,2$. This procedure yields

$$G(\mathbf{x}) = \frac{1}{4\pi}\left\{\frac{[1-(-1)^{x+y}]}{x+iy} + \frac{[(-1)^y-(-1)^x]}{x-iy}\right\}, \tag{29}$$

which exhibits the two sublattice structure that characterizes the square lattice problem. From this form we can recover the asymptotics of the dimer correlations established in Ref. 4. For example, the connected correlation function for two horizontal dimers displaced by $\mathbf{x}$ is given by the Grassmann expression

$$c_{xx}(\mathbf{x}) = \langle \psi(\mathbf{x})\psi(\mathbf{x}+\hat{\mathbf{x}})\psi(\mathbf{0})\psi(\hat{\mathbf{x}})\rangle - \psi(\mathbf{x})\psi(\mathbf{x}+\hat{\mathbf{x}})\rangle\langle\psi(\mathbf{0})\psi(\hat{\mathbf{x}})\rangle.$$

By Wick's theorem, $c_{xx} = -G^2(\mathbf{x}) + G(\mathbf{x}+\hat{\mathbf{x}})G(\mathbf{x}-\hat{\mathbf{x}})$ and using our asymptotic form for $G(\mathbf{x})$ we find

$$c_{xx}(\mathbf{x}) \sim \frac{(-1)^{x+y}}{4\pi^2}\left(\frac{1}{x+iy} + (-1)^y\frac{1}{x-iy}\right)^2, \tag{30}$$

where we have ignored constants in the denominators that generate subleading corrections in the generic case. For the special case of two dimers in the same column, separated by an even distance, this expression vanishes. However, even in that case one can recover the correct subleading form by reinstating the constants, as can be readily verified.

Next we consider adding in the diagonal bonds with fugacity t and find that near the nodes of S_0 it adds

$$S_p = it\sum_{\mathbf{x}} (-1)^y \psi(\mathbf{x})\psi(\mathbf{x}+\hat{\mathbf{x}}+\hat{\mathbf{y}})$$

$$= it\sum_{\mathbf{k}} \exp(-ik_x)\exp(-i(k_y-\pi))\tilde{\psi}_{\mathbf{k}}\tilde{\psi}_{-\mathbf{k}+\pi\hat{\mathbf{y}}}.$$

Expanding this near the nodes of the dispersion yields

$$S_p = 2it\int d^2\mathbf{x}(-\overline{\chi^1}\chi^1 + \overline{\chi^2}\chi^2), \tag{31}$$

i.e., two mass terms of opposite signs. This means that the model is invariant under the standard Kramers-Wannier duality of the Ising model, which sends $t\to -t$. Here this just interchanges the two fermions. It is easy to check that our Pfaffian analysis gives results independent of the sign of t. Changing $t\to -t$ leaves invariant the Green functions Q_s, and R_s for even s, while it flips the sign of R_s for odd s. This leaves all monomer and dimer correlators invariant.

It follows that perturbing away from the square lattice results in a non-analyticity in the thermodynamics, with behavior in the $d=2$ Ising universality class (with a doubling of the degrees of freedom). Specifically, Onsager's results for the Ising model give the dimer entropy density to be $\mathcal{S}(t) - \mathcal{S}(0) \propto -t^2\log t^2$, so that the model is indeed non-analytic at $t=0$. For t near zero, the correlation functions are now characterized by decay on the scale of $\xi \sim 1/t$, in agreement with our earlier, exact lattice computation [Eq. (19)].

It is interesting to ask where the order/disorder fields (σ/μ) of the Ising operator algebra appear in the lattice problem. The two known candidates here are the monomer and vison fields, both of which exhibit an inverse square root decay on the square lattice.[4,30] In the Ising model at the critical point, order and disorder two-point functions decay as $|\mathbf{x}|^{-1/4}$, so the monomer and vison fields must be bilinear in the order and disorder fields, as proven in Ref. 25. To narrow down the correspondence, we invoke four further constraints: (a) At $t=0$, the monomer-monomer correlator is nonzero only when the monomers are on different sublattices. (b) When $t\neq 0$, monomer correlators decay to a constant. (c) The vison-vison correlation function does not exhibit any sublattice structure and decays exponentially to zero when $t\neq 0$. (d) Under duality $t\to -t$, σ and μ change places in each of Majorana sectors. Because of the opposite signs in Eq. (31), one of the sectors is in the high-temperature phase, while the other is in a low-temperature phase. In an Ising low-temperature phase $\langle\sigma(\mathbf{x})\sigma(0)\rangle$ goes to a constant at large $|\mathbf{x}|$, while in a high-temperature phase $\langle\mu(\mathbf{x})\mu(0)\rangle$ goes to a constant. Thus for $t\neq 0$ only one of the four bilinears decays to a constant, either $\sigma^1\mu^2$ or $\sigma^2\mu^1$, where the superscripts refer to the two Majorana sectors. With these we can identify the monomer operators on the two sublattices with $\sigma^1\mu^2 \pm i\sigma^2\mu^1$; the relative $\pm i$ ensures that the correlator vanishes at $t=0$ when the monomers are on the same sublattice. In the absence of further constraints, the vison operator can be identified with either of the combinations $\sigma^1\sigma^2 \pm \mu^1\mu^2$. A fourth dimension 1/4 operator still needs to be identified to complete this set of identifications.

Finally, we should note that in the standard Ising model on the square lattice, equivalent to a dimer model on Fisher's lattice, things work somewhat differently, as we shall discuss elsewhere.[31] In that problem the two Ising phases correspond to confined/deconfined phases of the dimer problem.

VI. CONCLUDING REMARKS

We have shown that the classical model on a triangular lattice is generically in a liquid phase with deconfined monomers. This result contrasts with the critical correlations found on the bipartite square and honeycomb lattices. The more complicated, nonbipartite, Fisher lattice also exhibits a deconfined phase along with a confinement-deconfinement transition. It would clearly be interesting to see if other, as yet unstudied, examples follow this classification. In this context it is worth noting that the two critical dimer models admit height representations on account of their bipartite character—a feature often associated with criticality in two dimensions. It is also worth remarking that this correlation between criticality and bipartedness connects, via the quantum dimer model, to the Fradkin-Shenker theorem in lattice gauge theory.[32] Finally, for reasons noted in Sec. I, any further work along these lines would also be immediately useful in advancing our understanding of quantum magnetism.

Note added: After we submitted this paper, a preprint by A. Ioselevich, D.A. Ivanov, and M.V. Feigelman appeared

(cond-mat/0206451), who studied the triangular dimer correlations in the absence of monomers. Beyond the results reported here, they pointed out that the dimer correlation length depends on direction.

ACKNOWLEDGMENTS

We are grateful to Somendra Bhattacharjee and Bernard Nienhuis for their help with the literature on dimer models, and to Chris Henley for comments on the manuscript. R.M. would like to thank W. Krauth for useful discussions. This work was supported in part by NSF Grant DMR-0104799, a DOE OJI award, and a Sloan Foundation Fellowship (P.F.) and by NSF Grant No. DMR-9978074 and the David and Lucille Packard Foundation (S.L.S).

APPENDIX A: RECURSION RELATIONS

To obtain the recursion relations for the Green functions efficiently, it is helpful to do changes several of variables. First of all, we define $z \equiv \cos(2a)$. Since s is always odd, one can rewrite $2\cos(sa)\cos(a) = \cos[(s+1)a] + \cos[(s-1)a]$ in terms of powers of $\cos(2a)$. That is, we use the Chebyshev polynomials $T_j(y)$, which are defined by the relation $T_j[\cos(a)] = \cos(ja)$. For example, $T_1(y) = y$, $T_2(y) = 2y^2 - 1$, $T_3(y) = 4y^3 - 3y$, and so on; a closed-form expression can be found in Ref. 33. Using this gives

$$Q_s = \frac{1}{2\pi}\int_{-1}^{1} dz \frac{T_{(s+1)/2}(z) + T_{(s-1)/2}(z)}{\sqrt{(1-z^2)(7+4z+z^2)}}. \tag{A1}$$

This means that any Q_s can be expressed as a sum of the functions

$$U_k \equiv \frac{1}{2\pi}\int_{-1}^{1} dt \frac{z^k}{\sqrt{(1-z^2)(7+4z+z^2)}}$$

for $k = 1 \ldots (s+1)/2$. For example,

$$Q_1 = U_1 + U_0,$$

$$Q_3 = 2U_2 + U_1 - U_0,$$

$$Q_3 = 4U_3 - 3U_2 + 2U_1 - U_0,$$

$$Q_4 = 8U_4 + 4U_3 - 8U_2 - 3U_1 + U_0.$$

One also has

$$R_2 = 2U_1.$$

The reason we write things in terms of the U_i is that it is easy to derive recursion relations for them. This is useful because there are simple explicit expressions for the first few U_k. Denoting the denominator of (A1) as Y, the recursion relations follow from the fact that[33]

$$\frac{1}{Y}\left(m z^{m-1} Y^2 + \frac{1}{2} z^m \frac{d(Y^2)}{dz} \right) = \frac{d}{dz}(z^m Y)$$

is a total derivative. For our case, this yields the identity

$$(k-1)U_k + 2(2k-3)U_{k-1} + 6(k-2)U_{k-2} - 2(2k-5)U_{k-3} - 7(k-3)U_{k-4} = 0.$$

Even though the expressions for X_s and U_k look unwieldy, they can be made much nicer by a simple change of variable. Namely, defining $z = (\xi-4)/(\xi+2)$ yields

$$U_k = \frac{1}{4\pi}\int_1^\infty d\xi \left(\frac{\xi-4}{\xi+2}\right)^k \frac{1}{\sqrt{\xi^3-1}}. \tag{A2}$$

These turn out to be related to the complete elliptic integral $K(k)$ with $k = \sin(\pi/12)$, an integral whose properties were originally investigated by Legendre.[34] We can evaluate U_0 in terms of the β function as

$$U_0 = \frac{\Gamma(7/6)}{2\Gamma(2/3)\sqrt{\pi}} = 0.19326587782732139\ldots. \tag{A3}$$

Since $Q_1 = 1/6$, this yields immediately that

$$U_1 = 1/6 - U_0. \tag{A4}$$

This then gives us our first nontrivial Green function explicitly, because $R_2 = 2U_1 = -0.05319842232\ldots$. To utilize the recursion relations given above, we also need U_2. Using various properties of the complete elliptic integrals,[34] we have shown that remarkably enough, U_2 is simply related to the reciprocal of U_0, namely,

$$U_2 = U_0 + \frac{1}{4\pi\sqrt{3}U_0} - \frac{1}{3}. \tag{A5}$$

APPENDIX B: DERIVATION OF THE MATRIX FOR THE MONOMER CORRELATOR

The monomer-monomer correlator [Eq. (22)] is written in terms of matrices as

$$P^{(mm)}(p) = \mathrm{Pf}\,(M^{-1}M^{(mm)}).$$

We define

$$E \equiv M^{(mm)} - M.$$

Since by definition the Green's function $G_{jk} = (M^{-1})_{jk} = -\langle \psi_j \psi_k \rangle$, we have

$$P^{(mm)} = [\det(I + GE)]^{1/2},$$

where I is the identity. As seen from Eq. (22), there are three types of entries in E.

(1) We need to remove the links connected to the monomer sites 1 or $2p$. Thus $E_{jk} = -M_{jk}$ if either j or k is either 1 or $2p$.

(2) We need to change the sign on the links on the string. Thus $E_{jk} = -2M_{jk}$ if the link (jk) is part of the string.

(3) We need to account for the $\psi_1\psi_{2p}$ in Eq. (22). This is done by $E_{2p,1} = -E_{1,2p} = i$.

We now specialize to the case of monomers in adjacent rows a distance p apart. Here the matrix E has nonzero entries in $2(p+4)$ columns and rows. In E_{ab}, the indices r and

s run over $1 \ldots p$ for the sites in the lower row, and $p+1 \ldots 2p$ for the upper row. The remaining 8 columns and rows correspond to the sites surrounding the two monomers which are not part of the string; we denote those adjacent to the left monomer as $1',2',3',4'$, and those adjacent to the right monomer as $5',6',7',8'$.

Since we evaluated all the Green functions in Sec. III for $t=1$, at this point we could just plug in all the numbers, multiply the matrices, evaluate the determinant, and take the square root to get the monomer correlators. However, the determinant can be simplified a great deal, and is quite elegant. In fact, we can rewrite the correlator as a determinant of a matrix half the size.

Let us first consider the first column of $I+GE$. The non-zero entries of E_{b1} are when $b=2p$ or $b=2,p+1,1',2',3',4'$ (the latter sites surrounding the site 1). Note that $\Sigma_c G_{ac} M_{c1} = \delta_{a1}$ when c is summed over the sites around 1. Then

$$G_{ab}E_{b1} = iG_{a,2p} - \sum_c G_{ac}M_{c1} = G_{a,2p} - \delta_{a1}.$$

Thus

$$(I+GE)_{a1} = iG_{a,2p}.$$

Similarly, $(I+GE)_{a,2p} = -iG_{a1}$. We now consider the columns coming from the sites adjacent to site 1 but not part of the string. For these sites $c'=1',2',3',4'$, we have $E_{ab} \propto \delta_{a1}$. Thus in the kth column of $I+GE$ we have $G_{ab}E_{bc'} = G_{a1}E_{1c'}$. However, we can essentially remove this column without affecting the determinant. If we add the $2p$th column times $iE_{1c'}$ to the c'th column, the c'th column of $(I+GE)$ is just $\delta_{ac'}$. Thus the only non-zero entry in the c'th column is on the diagonal, and is 1. The determinant with these rows and columns removed is thus identical to those with these columns present. The rows and columns $5',6',7',8'$ are removed in a similar manner.

We denote the modified $2p \times 2p$ matrix (with the same Pfaffian) as $\mathcal{M}$. We can continue with such column manipulations to simplify the matrix further. Consider the pth column. We have

$$(I+GE)_{ap} = \delta_{ap} + 2iG_{a,2p-1} - itG_{a,2p}.$$

The last piece can be removed without changing the determinant by adding t times the first column of $\mathcal{M}$ to this column. This gives

$$\mathcal{M}_{ap} = \delta_{ap} + 2iG_{a,2p-1}.$$

Now consider the $p-1$th column:

$$(I+GE)_{a,p-1} = \delta_{a,p-1} + 2iG_{a,2p-2} - 2itG_{a,2p-1}.$$

We can simplify this by adding the t times the pth column to this, yielding, for the modified matrix,

$$\mathcal{M}_{a,p-1} = \delta_{a,p-1} + t\delta_{ap} + 2iG_{a,2p-2}.$$

Continuing in this fashion gives

$$\mathcal{M}_{ab} = \sum_{j=b}^{p} \delta_{aj} t^{a-b} + 2iG_{a,b+p-1}$$

for $b=2 \ldots p$ and $a=1 \ldots 2p$. We already have

$$\mathcal{M}_{a1} = iG_{a,2p}.$$

We can do the analogous manipulations for the columns $c=p+1 \ldots 2p-1$. This yields

$$\mathcal{M}_{ac} = \sum_{j=p+1}^{c} \delta_{aj} t^{c-a} - 2iG_{a,c-p+1}$$

and

$$\mathcal{M}_{a,2p} = -iG_{a,1}.$$

We can now write $\mathcal{M}$ in terms of the Q_s and R_s defined in the last section. For example,

$$\mathcal{M}_{a,2p} = \begin{cases} i(-1)^{[a/2]} Q_{1-a}, & 1 \leqslant a \leqslant p \\ (-1)^{[(a-p-1)/2]} R_{a-p}, & p+1 \leqslant a \leqslant 2p, \end{cases}$$

where $[x]$ is the greatest integer less than x. Putting this all together yields, for example, for $p=4$

$$\mathcal{M} = \begin{bmatrix} -R_4 & 2R_1 & 2R_2 & -2R_3 & 2iQ_1 & 0 & -2iQ_3 & 0 \\ -R_3 & 1-2R_0 & 2R_1 & 2R_2 & 0 & 2iQ_1 & 0 & -iQ_1 \\ R_2 & t-2R_{-1} & 1-2R_0 & 2R_1 & -2iQ_1 & 0 & 2iQ_1 & 0 \\ R_1 & t^2+2R_{-2} & t-2R_{-1} & 1-2R_0 & 0 & -2iQ_1 & 0 & iQ_3 \\ iQ_3 & 0 & -2iQ_1 & 0 & 1-2R_0 & t-2R_{-1} & t^2+2R_{-2} & R_1 \\ 0 & 2iQ_1 & 0 & -2iQ_1 & 2R_1 & 1-2R_0 & t-2R_{-1} & R_2 \\ -iQ_1 & 0 & 2iQ_1 & 0 & 2R_2 & 2R_1 & 1-2R_0 & -R_3 \\ 0 & -2iQ_3 & 0 & 2iQ_1 & -2R_3 & 2R_2 & 2R_1 & -R_4 \end{bmatrix},$$

where we have used the facts that $Q_{-s}=Q_s$ and $Q_s=0$ for s even. This matrix looks much nicer if we reshuffle rows and columns. We permute the first column through the others so that it becomes the pth column, and permute the $2p$th column through so that it becomes the $p+1$th column. This does not change the determinant. We then relabel the indices

$p+1 \ldots 2p$ in reverse order (i.e., interchange $2p \leftrightarrow p+1$, $2p-1 \leftrightarrow p+2$, etc.) We also multiply the pth and the $p+1$th columns by 2, so that we need to divide the resulting determinant by 4. These manipulations put the matrix into the form

$$\begin{pmatrix} \mathcal{R} & \mathcal{Q} \\ \mathcal{Q} & \mathcal{R} \end{pmatrix}, \tag{B1}$$

where $\mathcal{R}$ and $\mathcal{Q}$ are the $p \times p$ matrices defined by

$$\mathcal{R}_{ij} = (-1)^{[(j-i)/2]} 2R_{j-i+1} + \theta(i-j) t^{i-j-1}, \tag{B2}$$

$$\mathcal{Q}_{ij} = i(-1)^{[(j+i)/2]} 2Q_{p+1-i-j}, \tag{B3}$$

where $\theta(x)=1$ for $x>0$ and 0 for $x \leqslant 0$. For example, for $p=6$ we have

$$\mathcal{R} = \begin{pmatrix} 2R_1 & 2R_2 & -2R_3 & -2R_4 & 2R_5 & 2R_6 \\ 1-2R_0 & 2R_1 & 2R_2 & -2R_3 & -2R_4 & 2R_5 \\ t-2R_{-1} & 1-2R_0 & 2R_1 & 2R_2 & -2R_3 & -2R_4 \\ t^2+2R_{-2} & t-2R_{-1} & 1-2R_0 & 2R_1 & 2R_2 & -2R_3 \\ t^3+2R_{-3} & t^2+2R_{-2} & t-2R_{-1} & 1-2R_0 & 2R_1 & 2R_2 \\ t^4-2R_{-4} & t^3-2R_{-3} & t^2+2R_{-2} & t-2R_{-1} & 1-2R_0 & 2R_1 \end{pmatrix}$$

$$\mathcal{Q} = \begin{pmatrix} 2iQ_5 & 0 & -2iQ_3 & 0 & 2iQ_1 & 0 \\ 0 & -2iQ_3 & 0 & 2iQ_1 & 0 & -2iQ_1 \\ -2iQ_3 & 0 & 2iQ_1 & 0 & -2iQ_1 & 0 \\ 0 & 2iQ_1 & 0 & -2iQ_1 & 0 & 2iQ_3 \\ 2iQ_1 & 0 & -2iQ_1 & 0 & 2iQ_3 & 0 \\ 0 & -2iQ_1 & 0 & 2iQ_3 & 0 & -2iQ_5 \end{pmatrix}$$

The determinant of matrices of the form (B1) can be simplified:[35]

$$\det\begin{pmatrix} \mathcal{R} & \mathcal{Q} \\ \mathcal{Q} & \mathcal{R} \end{pmatrix} = \det\begin{pmatrix} \mathcal{R}+\mathcal{Q} & \mathcal{Q} \\ \mathcal{Q}+\mathcal{R} & \mathcal{R} \end{pmatrix} = \det\begin{pmatrix} \mathcal{R}+\mathcal{Q} & \mathcal{Q} \\ 0 & \mathcal{R}-\mathcal{Q} \end{pmatrix}$$
$$= \det(\mathcal{R}+\mathcal{Q}) \det(\mathcal{R}-\mathcal{Q}).$$

In our case, the latter two determinants are the same, because $\mathcal{R}$ is symmetric around the off-diagonal (the diagonal from upper right to lower left), while $\mathcal{Q}$ is antisymmetric around the off-diagonal. Thus

$$\det \mathcal{M} = \frac{1}{4} [\det(\mathcal{R}+\mathcal{Q})]^2.$$

This yields result (23) for the monomer-monomer correlator above.

[1] P. W. Kasteleyn, Physica (Amsterdam) **27**, 1209 (1961); J. Math. Phys. **4**, 287 (1963).

[2] M. E. Fisher, J. Math. Phys. **7**, 1776 (1966).

[3] For a review, see J. F. Nagle, C. S. O. Yokio, and S. M. Bhattacharjee, in *Phase Transitions and Critical Phenomena*, edited by C. Domb and J. Lebowitz (Academic Press, New York, 1980), Vol. 13.

[4] M. E. Fisher and J. Stephenson, Phys. Rev. **132**, 1411 (1963).

[5] B. M. McCoy and T. T. Wu, *The Two-Dimensional Ising Model* (Harvard University Press, Cambridge, MA, 1973).

[6] P. W. Anderson, Science **235**, 1196 (1987).

[7] D. S. Rokhsar and S. A. Kivelson, Phys. Rev. Lett. **61**, 2376 (1988).

[8] The precise connection between classical and quantum correlations requires additional assumptions about the ergodicity of the quantum dimer Hamiltonian in the space of dimer configurations (Refs. 7 and 9). This problem was addressed for a finite triangular lattice with open boundary conditions in C. Kenyon and E. Remila, Discrete Math. **152**, 191 (1996).

[9] R. Moessner and S. L. Sondhi, Phys. Rev. Lett. **86**, 1881 (2001).

[10] F. Y. Wu, Phys. Rev. **168**, 539 (1967).

[11] X. G. Wen, Phys. Rev. B **40**, 7387 (1989); Int. J. Mod. Phys. B **4**, 239 (1990); X. G. Wen and Q. Niu, Phys. Rev. B **41**, 9377 (1990).

[12] R. Moessner, S. L. Sondhi, and E. Fradkin, Phys. Rev. B **65**, 024504 (2002).

[13] J. F. Nagle, Phys. Rev. **152**, 190 (1966).
[14] D. S. Gaunt, Phys. Rev. **179**, 174 (1969).
[15] S. Samuel, J. Math. Phys. **21**, 2806 (1980).
[16] F. Mila, Phys. Rev. Lett. **81**, 2356 (1998).
[17] W. F. Wolff and J. Zittartz, Z. Phys. B: Condens. Matter **B49**, 139 (1982).
[18] An actual magnetic model will exhibit a finite density of spinons as a finite temperature. Our diagnostic is the equivalent of the ''Polyakov loop'' for gauge theories *without* dynamical matter, at finite temperatures. The latter measures the free energy of two static quarks at varying separations.
[19] This problem was concurrently studied numerically (by Monte Carlo simulations and by exact enumeration) by W. Krauth and R. Moessner, cond-mat/0206177 (unpublished).
[20] M. E. Fisher, Phys. Rev. **124**, 1664 (1961).
[21] M. E. Fisher and H. N. V. Temperley, Philos. Mag. **6**, 1061 (1961).
[22] The corresponding expression for g in Ref. 9 contains an error in the sign of the argument of the first exponential, which is corrected here.
[23] R. E. Hartwig, J. Math. Phys. **7**, 286 (1966).
[24] R. Moessner and S. L. Sondhi, Phys. Rev. B **62**, 14 122 (2000).
[25] H. Au-Yang and J. H. H. Perk, Phys. Lett. A **104**, 131 (1984).
[26] N. Read and B. Chakraborty, Phys. Rev. B **40**, 7133 (1989).
[27] S. Kivelson, Phys. Rev. B **39**, 259 (1989).
[28] L. Balents, M. P. A. Fisher, and S. M. Girvin, Phys. Rev. B **65**, 224412 (2002).
[29] K. Shtengel (private communication).
[30] G. Forgacs, Phys. Rev. B **22**, 4473 (1980).
[31] R. Moessner and S. L. Sondhi (unpublished).
[32] E. H. Fradkin and S. H. Shenker, Phys. Rev. D **19**, 3682 (1979).
[33] A. Erdelyi, *Bateman Manuscript Project: Higher Transcendental Functions* (McGraw-Hill, New York, 1953), Vol. 2.
[34] E. T. Whitaker and G. N. Watson, *A Course in Modern Analysis* (Cambridge University Press, Cambridge, 1927).
[35] We thank Michael Fowler for providing this proof.